



Synthesis, Crystal Structure and Hirshfeld Surface Analysis of 3,14-Dimethyl-2,6,13,17-tetraazatricyclo(16.4.0.0^{7,12})docosane-2-(nitric acid)

DOHYUN MOON¹, SUNGHWAN JEON², KEON SANG RYOO² and JONG-HA CHOI^{2*}

¹Beamline Department, Pohang Accelerator Laboratory, Pohang 37673, Republic of Korea

²Department of Chemistry, Andong National University, Andong 36729, Republic of Korea

*Corresponding author: E-mail: jhchoi@anu.ac.kr

Received: 19 October 2019;

Accepted: 9 December 2019;

Published online: 31 January 2020;

AJC-19780

The crystal structure of 3,14-dimethyl-2,6,13,17-tetraazatricyclo(16.4.0.0^{7,12})docosane-2-(nitric acid), C₂₀H₄₀N₄·2(NO₂OH) had been determined using synchrotron radiation at 220 K. The compound crystallized in the space group P2₁/n of the monoclinic system with two mononuclear formula units in a cell of dimensions a = 9.1930(18), b = 10.120(2), c = 12.979(3) Å and β = 101.06(3)°. The asymmetric unit contains half a centrosymmetric macrocycle and one nitric acid molecule. There were two molecules in the unit cell. In structure of macrocycle, C-C and N-C bond lengths were in the range 1.5198(19) to 1.5367(18) Å and 1.4744(16) to 1.4986(16) Å, respectively. The NO₂OH group has one longer N-O bond of 1.3441(18) Å and two shorter N-O bond of 1.2509(19) Å and 1.2510(19) Å, and O-N-O angles of 126.31(14)°, 117.98(14)° and 115.71(14)°. The N-H...O and N-H...N hydrogen bonds interconnect macrocycle (C₂₀H₄₀N₄) with nitric acid molecules while two O-H...O hydrogen bonds link the nitric acid molecule to neighboring nitric acid molecule each other. The molecule was stabilized by forming intermolecular N-H...O, N-H...N and O-H...O hydrogen bonds. Hirshfeld surface analysis by 3D molecular surface contours and 2D fingerprint plots have been used to analyze intermolecular interactions present in the crystal.

Keywords: Crystal structure, Macrocycle, Nitric acid, Hydrogen bonds, Synchrotron radiation, Hirshfeld surface analysis.

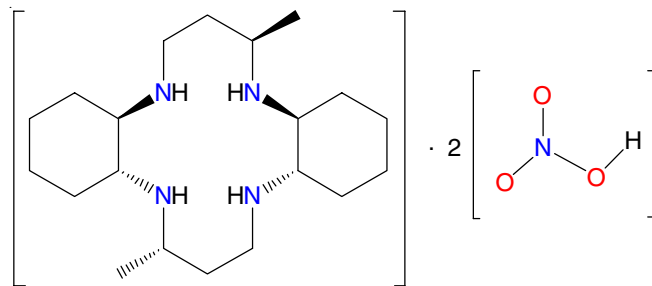
INTRODUCTION

1,4,8,11-Tetraazacyclotetradecane (cyclam) derivatives and their transition metal complexes have been reported to exhibit anti-HIV effects and stimulate stem cell activity in bone marrow [1-3]. The structure of 14-membered tetraaza macrocycle is flexible and can adopt both planar (*trans*) and folded (*cis*)-configurations. A total of five conformational *trans*-isomers can be adopted, which differ in the chirality of *sec*-NH centers. The *trans*-I, *trans*-II and *trans*-V conformations can fold to form *cis*-I, *cis*-II and *cis*-V isomers, respectively [4-6]. The macrocycle conformation and orientations of N-H bonds are very important for CXCR4 chemokine receptor recognition [1-3]. Therefore, understanding of the coordination behaviour and conformation of this cyclam derivative has become important for improved design and development of novel and highly effective anti-HIV drugs. Macrocycle 3,14-dimethyl-2,6,13,17-tetraazatricyclo(16.4.0.0^{7,12})docosane (C₂₀H₄₀N₄, L) contains a cyclam backbone with two cyclohexane subunits and two

methyl groups. The crystal structures of [Cu(L)](NO₃)₂·3H₂O, [Cu(L)](NO₃)₂, [Cu(L)](ClO₄)₂ and [Cu(L)(H₂O)₂](BF₄)₂·2H₂O together with [Zn(L)(OCOCH₃)₂] have been reported [7-11]. In these structures, copper(II) or zinc(II) cations have tetragonal geometry with four N atoms of the macrocyclic ligand in equatorial position and O atom of counter-anion, water molecule or acetato ligand in axial position. In these Cu(II) and Zn(II) complexes, macrocyclic ligand adopts the most stable *trans*-III conformation. The crystal structures of (C₂₀H₄₀N₄)·2C₁₁H₁₀O [12], [C₂₀H₄₂N₄](SO₄)·2MeOH [13] and [C₂₀H₄₄N₄]-Cl₄·4H₂O [14] have also been reported. As part of our extensive research program in this research area, we herein reported the synthesis of compound, C₂₀H₄₀N₄·2(NO₂OH) (**Scheme-I**), its Hirshfeld Surface analysis and structural characterization by synchrotron single-crystal X-ray diffraction.

EXPERIMENTAL

Synthesis: Commercially available *trans*-1,2-cyclohexanediamine, methyl vinyl ketone and silver nitrite (Sigma-Aldrich)



Scheme-I: Chemical structure of $C_{20}H_{40}N_4 \cdot 2(NO_2OH)$ (**I**)

were used as provided. All the chemicals were of reagent grade and used without further purification. As a starting material, 3,14-dimethyl-2,6,13,17-tetraazatricyclo(16.4.0.0^{7,12})-docosane (**L**) was prepared according to a published procedure [15]. A solution of macrocyclic ligand (**L**) (0.33 g, 1.0 mmol) in methanol 10 mL was added to a stirred solution of $AgNO_2$ (0.34 g, 2.2 mmol) in water 10 mL. The resulting solution was filtered off. The orange filtrate was allowed in an open beaker protected from light at room temperature. Pale yellow crystals of compound (**I**) suitable for X-ray analysis were obtained from the solution over a period of a few weeks.

X-ray structural determination: A block pale yellow crystal (0.18 mm × 0.17 mm × 0.14 mm) of the title compound was coated with Parabar 10312 (Hampton Research Inc.) to mount micro-loop. The diffraction data were measured on an ADSC Quantum-210 detector at BL2D-SMC with a silicon (111) double-crystal monochromator (0.610 Å) at Pohang Accelerator Laboratory, Korea using synchrotron radiation and a nitrogen cold stream. The PAL BL2D-SMDC program [16] was used for data collection and HKL3000sm (Ver. 716.7) [17] was used for cell refinement, reduction and absorption correction. The structure was solved by the intrinsic phasing method with SHELXT program [18] and refined by full-matrix least-squares calculations with the SHELXL program [18]. Molecular graphics were produced using DIAMOND-3 [19]. Crystal data, data collection and structure refinement details are summarized in Table-1. All the C and N-bound H atoms in compound were placed in geometrically idealized positions and constrained to ride on their parent atoms, with C-H distances of 0.97–0.99 Å with $U_{iso}(H)$ values of 1.2 and 1.5 U_{eq} of the parent atoms respectively. The N-bound H atoms of $C_{20}H_{42}N_4$ and the O-bound H atoms of the nitric acid molecules were located in a difference Fourier map and refined isotropically, with the N-H distance restrained using DFIX (0.90 Å) and the O-H distances restrained using DFIX (0.84 Å), respectively and with $U_{iso}(H)$ values of 1.2 U_{eq} of the parent atoms. Two reflections with $F_o \gg F_c$, were omitted from the final refinement cycles.

RESULTS AND DISCUSSION

Crystallographic structure: The title compound of uncharged macrocycle and two nitric acid molecules was prepared during study of macrocyclic ligand and its silver(II) complex. The structure analysis showed the monoclinic space group of $P2_1/n$ with $Z = 2$. An ellipsoid plot of the compound together with the atom-numbering scheme is shown in Fig. 1. The asymmetric unit contains one half of macrocycle, which lies about a center of inversion and one neutral nitric acid molecule. The

TABLE-1
CRYSTALLOGRAPHIC DATA FOR COMPOUND **I**

Crystal data	
Chemical formula	$C_{20}H_{40}N_4 \cdot 2(NO_3H)$
M_r	462.59
Crystal system, space group	Monoclinic, $P2_1/n$
Temperature (K)	217
a, b, c (Å)	9.1930 (18), 10.120 (2), 12.979 (3)
β (°)	101.06 (3)
V (Å ³)	1185.1 (4)
Z	2
Radiation type	Synchrotron, $\lambda = 0.610$ Å
μ (mm ⁻¹)	0.07
Crystal size (mm)	0.18 × 0.17 × 0.14
Data collection	
Diffractometer	Rayonix MX225HS CCD area detector
Absorption correction	Empirical (using intensity measurements) HKL3000sm SCALEPACK [17]
T_{min} , T_{max}	0.829, 1.000
No. of measured, independent and observed [$I > 2\sigma(I)$] reflections	
R_{int}	0.066
$(\sin \theta/\lambda)_{max}$ (Å ⁻¹)	0.693
Refinement	
$R[F^2 > 2\sigma(F^2)]$, $wR(F^2)$, S	0.074, 0.223, 1.08
No. of reflections	3270
No. of parameters	155
No. of restraints	3
H-atom treatment	H atoms treated by a mixture of independent and constrained refinement
$\Delta\rho_{max}$, $\Delta\rho_{min}$ (e Å ⁻³)	1.47, -0.97

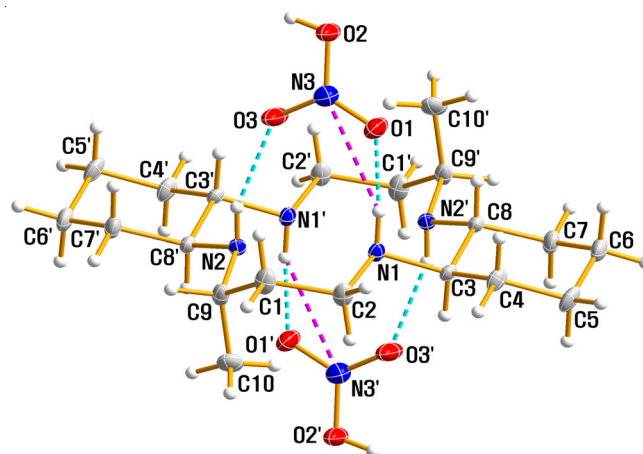


Fig. 1. Molecular structure of compound **I**, drawn with displacement ellipsoids at the 50 % probability level. Dashed lines represent hydrogen bonding interactions and primed atoms are related by the symmetry code (1-x, 1-y, 1-z)

four N atoms are coplanar and the two methyl substituents are anti with respect to the macrocyclic plane as a result of the molecular inversion symmetry. Selected bond lengths and angles and their standard deviations are given in Table-2.

A six-membered cyclohexane ring adopts a stable chair conformation. Within the centrosymmetric macrocycle $C_{20}H_{42}N_4$, the C-C and N-C bond lengths were varied from 1.5198(19) to 1.5367(18) Å and from 1.4744(16) to 1.4986(16) Å, respectively. The range of N-C-C and C-N-C angles is 108.02(10) to

TABLE-2
SELECTED BOND DISTANCES (Å) AND
ANGLES (°) FOR COMPOUND I

O1–N3	1.2509 (19)	C1–C9	1.532 (2)
O2–N3	1.3441 (18)	C4–C5	1.530 (2)
O3–N3	1.2510 (19)	C5–C6	1.521 (2)
N1–C2	1.4902 (17)	C6–C7	1.528 (2)
N1–C3	1.4986 (16)	C7–C8	1.5367 (18)
N2–C8 ⁱ	1.4718 (16)	C9–C10	1.525 (2)
N2–C9	1.4744 (16)	C3–C4	1.5280 (18)
C1–C2	1.5198 (19)	C3–C8	1.5290 (18)
O1–N3–O3	126.31 (14)	N2–C9–C10	109.77 (12)
O1–N3–O2	115.71 (14)	N2–C9–C1	109.19 (11)
O3–N3–O2	117.98 (14)	C2–C1–C9	116.34 (12)
C2–N1–C3	114.60 (10)	C3–C4–C5	109.71 (12)
C8 ⁱ –N2–C9	115.22 (10)	C3–C8–C7	110.25 (10)
N1–C2–C1	111.68 (11)	C4–C3–C8	112.04 (11)
N1–C3–C4	111.35 (11)	C5–C6–C7	110.25 (12)
N1–C3–C8	108.51 (10)	C6–C5–C4	110.28 (12)
N2 ⁱ –C8–C3	108.02 (10)	C6–C7–C8	111.99 (12)
N2 ⁱ –C8–C7	113.88 (11)	C10–C9–C1	113.33 (12)
C3–N1–C2–C1	-166.31 (12)	C4–C3–C8–N2 ⁱ	179.32 (10)
C9–C1–C2–N1	63.92 (17)	N1–C3–C8–C7	177.67 (10)
C2–N1–C3–C4	-55.28 (15)	C4–C3–C8–C7	54.31 (14)
C2–N1–C3–C8	-179.05 (11)	C6–C7–C8–N2 ⁱ	-175.29 (11)
N1–C3–C4–C5	-179.07 (11)	C6–C7–C8–C3	-53.70 (15)
C8–C3–C4–C5	-57.34 (15)	C8 ⁱ –N2–C9–C10	68.61 (14)
C3–C4–C5–C6	59.17 (16)	C8 ⁱ –N2–C9–C1	-166.60 (11)
C4–C5–C6–C7	-58.91 (16)	C2–C1–C9–N2	-69.69 (16)
C5–C6–C7–C8	56.48 (16)	C2–C1–C9–C10	53.00 (17)
N1–C3–C8–N2 ⁱ	-57.33 (13)	–	–

Symmetry code: (i) $-x+1, -y+1, -z+1$.

113.88(11)° and 114.60 (10) to 115.22 (10)°, respectively. The bond lengths and angles within the free C₂₀H₄₀N₄ are comparable to those found in (C₂₀H₄₀N₄)·2C₁₁H₁₀O [12], [C₂₀H₄₂N₄](SO₄)·2MeOH [13] and [C₂₀H₄₄N₄]Cl₄·4H₂O [14]. The nitrate groups geometrical arrangement with one longer N–O bond of 1.3441(18) Å and two shorter N–O bond of 1.2509(19) Å and 1.2510(19) Å, and O–N–O angles of 126.31(14)°, 117.98(14)° and 115.71(14)°, corresponds with that of an HNO₃ molecule [15] rather than geometry of a nitrate ion [20].

Supramolecular features: Extensive N–H···O, O–H···O and N–H···N hydrogen-bonding interactions occur in the crystal structure (Table-3). The crystal packing diagram along the *b*-axis is shown in Fig. 2. The O–H···O hydrogen bonds link the nitric acid molecule to neighbouring the nitric acid molecule each other, while N–H···O and N–H···N hydrogen bonds interconnect macrocycle (C₂₀H₄₀N₄) with nitric acid molecules. The

TABLE-3
HYDROGEN BOND PARAMETERS (Å, °) FOR COMPOUND I

D–H···A	D–H	H···A	D···A	D–H···A
O2–H1O···O3 ⁱ	0.84 (1)	1.84 (1)	2.6618 (18)	166 (3)
N1–H1N···O1	0.90 (1)	1.79 (1)	2.6892 (17)	173 (2)
N1–H1N···N3	0.90 (1)	2.61 (1)	3.4024 (19)	148 (2)
N2–H2N···O3	0.90 (1)	2.06 (1)	2.9165 (17)	157 (2)

Symmetry code: (i) $-x+2, -y+1, -z+1$.

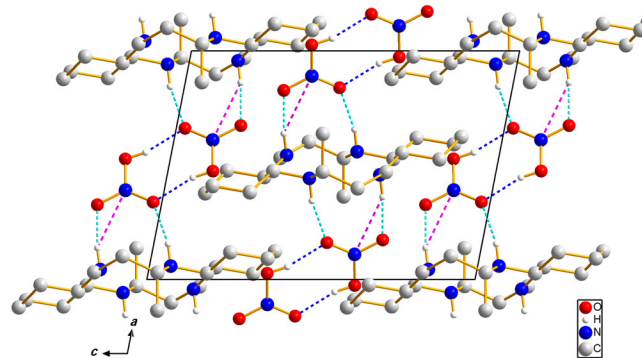


Fig. 2. Crystal packing in compound I, viewed perpendicular to the *ac* plane. Dashed lines represent N–H···O (cyan), N–H···N (pink) and O–H···O (blue) hydrogen bonding interactions, respectively. H atoms bound to C have been omitted

crystal structure is stabilized by molecular hydrogen bonds involving the macrocycle N–H groups and nitric acid molecule O–H groups as donors, and the O or N atoms of nitric acid molecules as acceptors, giving rise to a three-dimensional network (Figs. 1 and 2).

Hirshfeld surface analysis: By using Hirshfeld surface [21], close contacts of a structure of intermolecular can be visualized and explored. Hirshfeld surface is a useful tool by using Crystal Explorer [22] for describing the surface characteristics of the molecules. The three-dimensional d_{norm} surface shows negative values for a shorter intermolecular contact and positive values for a longer one than the sum of van der Waals radii [21,23]. The molecular Hirshfeld surface d_{norm} surface, shape index and curvedness are shown in Fig. 3.

The d_{norm} surface shows identification of very close intermolecular interactions. On contrary, the shape index is the most sensitive to very delicate changes in surface shape. The curvedness provides the shape of molecules. The flat areas of the surface stand for the low values of curvedness while the sharp ones indicate the high values of it. And the surface is usually divided into patches for indicating interactions between

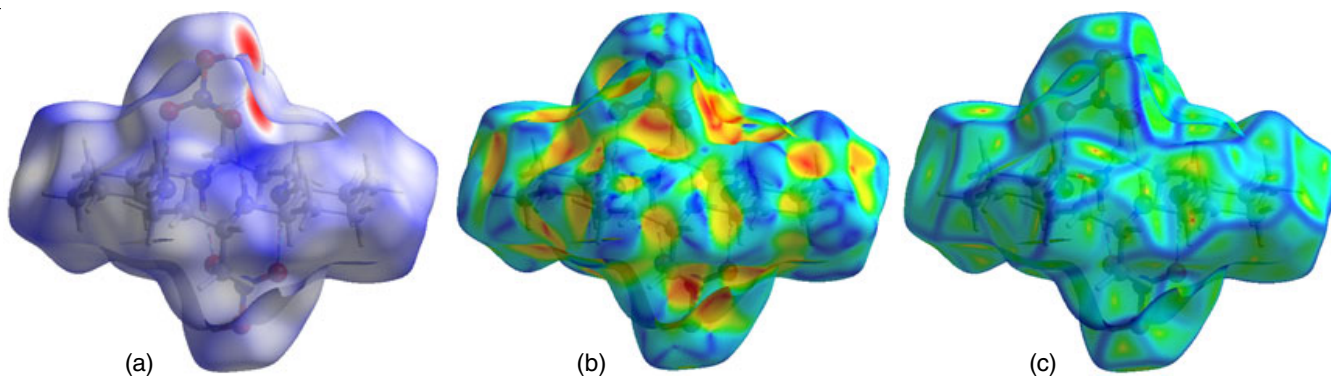


Fig. 3. Hirshfeld surfaces mapped with (a) d_{norm} , (b) shape-index and (c) curvedness

neighboring molecules. The d_{norm} surface shows the red and white spots for main contacts due to H...O, H...H and H...N interactions. The 2-D fingerprint plots [23] in the Crystal Explorer give information regarding the intermolecular contacts and their percentage distributions on the Hirshfeld surface. Hirshfeld surface contours and 2D fingerprint plots of various interactions are shown in Figs. 4-7, respectively. The d_i is the closet internal distance from a given point on the Hirshfeld surface and d_e is the closest external contact [24-28].

Conclusion

A newly prepared compound, $\text{C}_{20}\text{H}_{40}\text{N}_4 \cdot 2(\text{NO}_2\text{OH})$ has been characterized by single-crystal X-ray diffraction and Hirshfeld surface analyses. The asymmetric unit contains half

a centrosymmetric macrocycle and one nitric acid molecule. In the structure of macrocycle, the C-C and N-C bond lengths are in the range 1.5198(19) to 1.5367(18) Å and 1.4744(16) to 1.4986(16) Å, respectively. The NO_2OH group has one longer N-O bond of 1.3441(18) Å and two shorter N-O bond of 1.2509(19) Å and 1.2510(19) Å, and O-N-O angles of 126.31(14)°, 117.98(14)° and 115.71(14)°. The N-H...O and N-H...N hydrogen bonds interconnect macrocycle with nitric acid molecules while two O-H...O hydrogen bonds link the nitric acid molecule to neighbouring the nitric acid molecule each other. The molecule is stabilized by the intermolecular N-H...O, N-H...N and O-H...O hydrogen bonds. Hirshfeld surface analysis represents that the H...H, H...O/O...H and H...N/N...H contacts were the major molecular interactions in compound **I**.

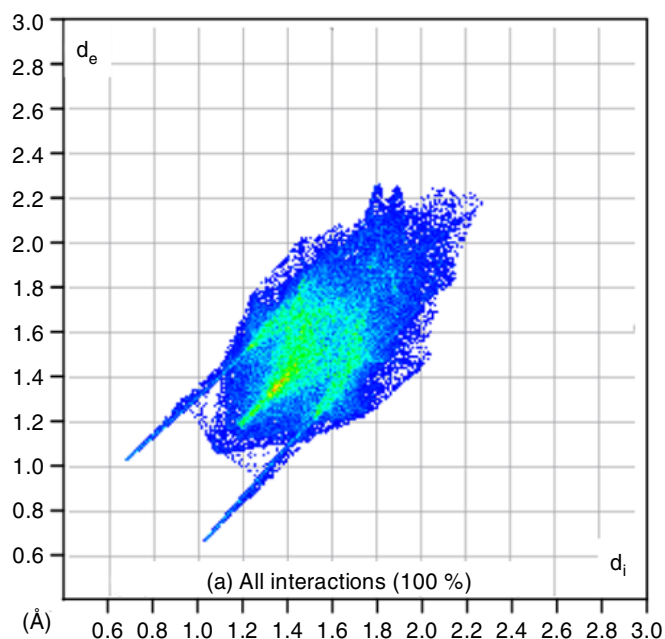
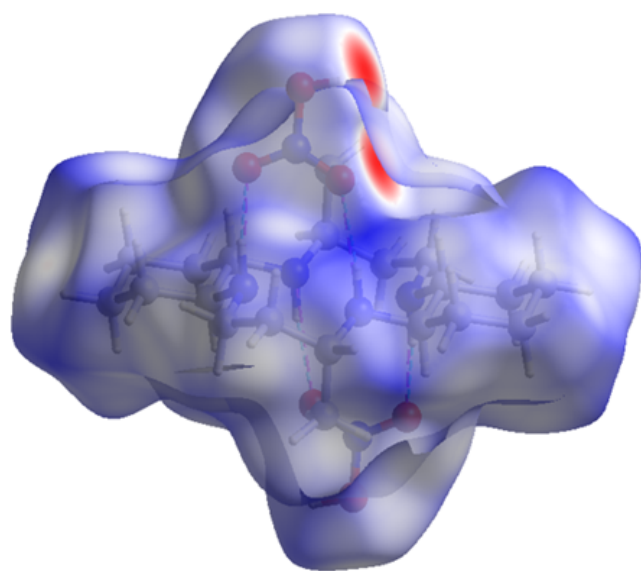


Fig. 4. Hirshfeld surface mapped with (left) d_{norm} and 2D fingerprint map (right) for all interactions

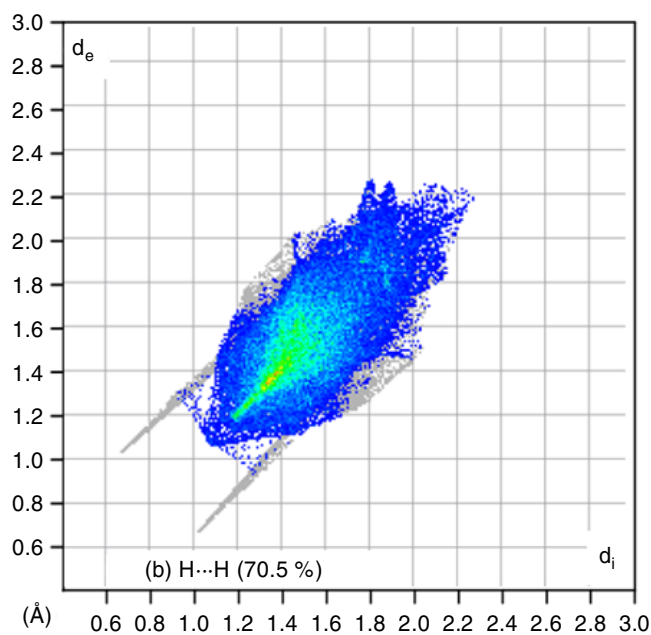
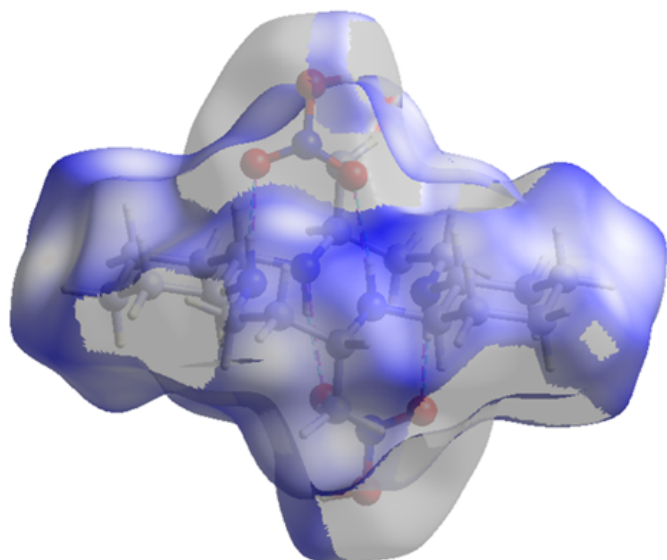


Fig. 5. Hirshfeld surface mapped with (left) d_{norm} and 2D fingerprint plot (right) for H...H interaction

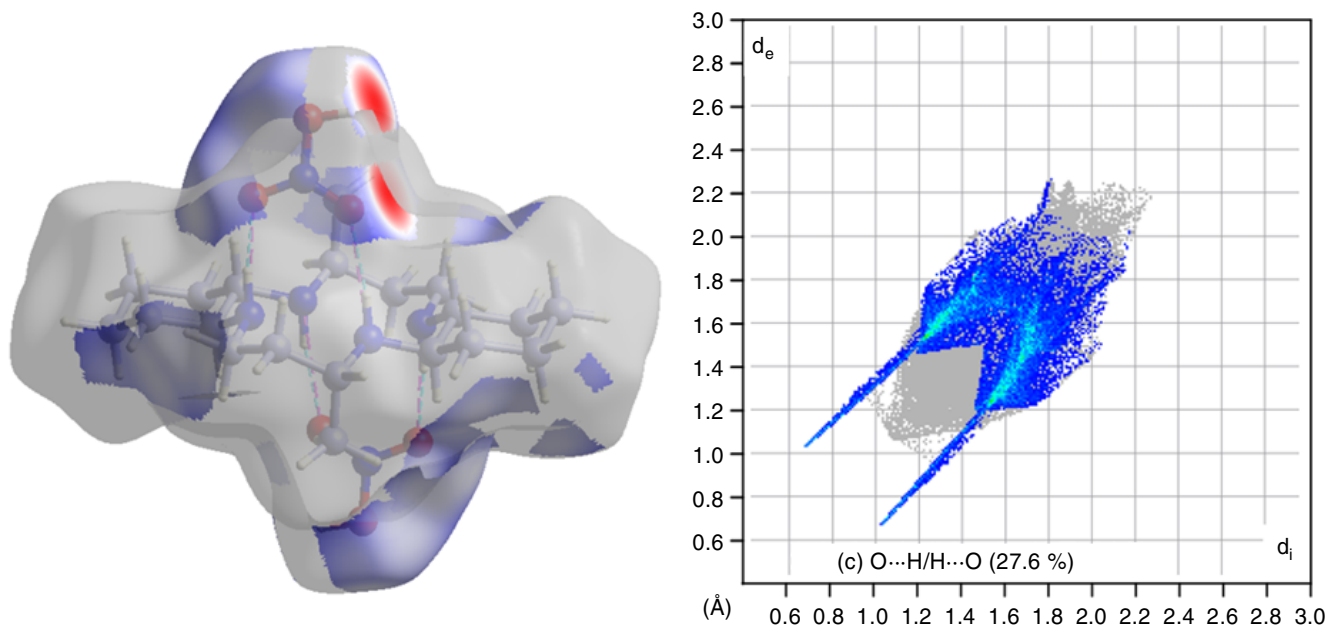


Fig. 6. Hirshfeld surface mapped with (left) d_{norm} and 2D fingerprint plot (right) for H...O/O...H interactions

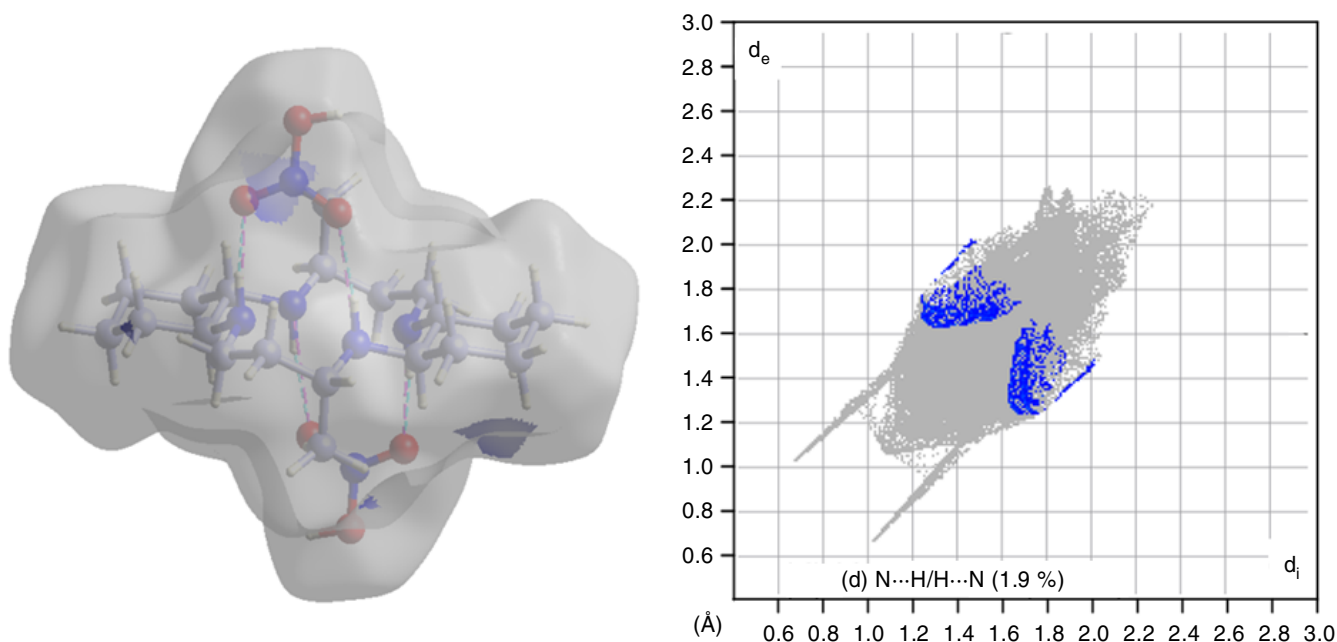


Fig. 7. Hirshfeld surface mapped with (left) d_{norm} and 2D fingerprint plot (right) for H...N/N...H interactions

Supplementary material

Crystallographic data for the structures reported here have been deposited with CCDC Deposition No 1960250. These data can be obtained free of charge from the Cambridge Crystallographic Data Centre, 12 Union Road, Cambridge CB2 1EZ, UK, Fax: +441223336033; E-mail: deposit@ccdc.cam.ac.uk.

ACKNOWLEDGEMENTS

This work was supported by a Research Grant of Andong National University. The X-ray crystallography experiment at PLS-II BL2D-SMC beamline was supported in part by MSICT and POSTECH.

CONFLICT OF INTEREST

The authors declare that there is no conflict of interests regarding the publication of this article.

REFERENCES

- G.C. Valks, G. McRobbie, E.A. Lewis, T.J. Hubin, T.M. Hunter, P.J. Sadler, C. Pannecouque, E. De Clercq and S.J. Archibald, *J. Med. Chem.*, **49**, 6162 (2006); <https://doi.org/10.1021/jm0607810>
- L. Ronconi and P.J. Sadler, *Coord. Chem. Rev.*, **251**, 1633 (2007); <https://doi.org/10.1016/j.ccr.2006.11.017>
- E. De Clercq, *J. Med. Chem.*, **53**, 1438 (2010); <https://doi.org/10.1021/jm900932g>

4. J.-H. Choi, *Inorg. Chim. Acta*, **362**, 4231 (2009); <https://doi.org/10.1016/j.ica.2009.05.024>
5. M.A. Subhan, J.-H. Choi and S.W. Ng, *Z. Anorg. Allg. Chem.*, **637**, 2193 (2011); <https://doi.org/10.1002/zaac.201100423>
6. J. Moncol, M. Mazúr, M. Valko, K.S. Ryoo and J.-H. Choi, *J. Mol. Struct.*, **1202**, 127224 (2020); <https://doi.org/10.1016/j.molstruc.2019.127224>
7. J.-H. Choi, T. Suzuki and S. Kaizaki, *Acta Crystallogr. E*, **62**, m2383 (2006); <https://doi.org/10.1107/S1600536806034234>
8. J.-H. Choi, K.S. Ryoo and K.-M. Park, *Acta Crystallogr. E*, **63**, m2674 (2007); <https://doi.org/10.1107/S1600536807048039>
9. J.-H. Choi, T. Joshi and L. Spiccia, *Z. Anorg. Allg. Chem.*, **638**, 146 (2012); <https://doi.org/10.1002/zaac.201100398>
10. J.-H. Choi, M.A. Subhan and S.W. Ng, *Acta Crystallogr. E*, **68**, m190 (2012); <https://doi.org/10.1107/S1600536812001845>
11. A. Ross, J.-H. Choi, T.M. Hunter, C. Pannecouque, S.A. Moggach, S. Parsons, E. De Clercq and P.J. Sadler, *Dalton Trans.*, **41**, 6408 (2012); <https://doi.org/10.1039/c2dt30140g>
12. J.-H. Choi, M.A. Subhan, K.S. Ryoo and S.W. Ng, *Acta Crystallogr. E*, **68**, o102 (2012); <https://doi.org/10.1107/S160053681105272X>
13. F. White, P.J. Sadler and M. Melchart, CSD Communication CCDC 1408165 (2015).
14. G.B. Richter-Addo, *Acta Crystallogr. E*, **74**, 1039 (2018); <https://doi.org/10.1107/S2059798318014997>
15. M.D. Moran, D.S. Brock, H.P.A. Mercier and G.J. Schrobilgen, *J. Am. Chem. Soc.*, **132**, 13823 (2010); <https://doi.org/10.1021/ja105618w>
16. J.W. Shin, K. Eom and D. Moon, *J. Synchrotron Rad.*, **23**, 369 (2016); <https://doi.org/10.1107/S1600577515021633>
17. Z. Otwinowski and W. Minor, eds., C.W. Carter Jr. and R.M. Sweet, *Methods in Enzymology*, Academic Press: New York, vol. 276, *Macromolecular Crystallography, Part A*, p. 307 (1997).
18. G.M. Sheldrick, *Acta Crystallogr. A*, **71**, 3 (2015); <https://doi.org/10.1107/S2053273314026370>
19. K. Brandenburg and H. Putz, DIAMOND-3, University of Bonn, Bonn Germany (2014).
20. D. Moon and J.-H. Choi, *Acta Crystallogr. E*, **74**, 461 (2018); <https://doi.org/10.1107/S2056989018003560>
21. M.A. Spackman and D. Jayatilaka, *CrystEngComm*, **11**, 19 (2009); <https://doi.org/10.1039/B818330A>
22. M.J. Turner, J.J. McKinnon, S.K. Wolff, D.J. Grimwood, P.R. Spackman, D. Jayatilaka and M.A. Spackman, *CrystalExplorer17*, University of Western Australia (2017).
23. M.A. Spackman and J.J. McKinnon, *CrystEngComm*, **4**, 378 (2002); <https://doi.org/10.1039/B203191B>
24. D. Moon, S. Tanaka, T. Akitsu and J.-H. Choi, *J. Mol. Struct.*, **1154**, 338 (2018); <https://doi.org/10.1016/j.molstruc.2017.10.066>
25. T. Aree, Y.P. Hong and J.-H. Choi, *J. Mol. Struct.*, **1163**, 86 (2018); <https://doi.org/10.1016/j.molstruc.2018.02.102>
26. S. Jeon, J. Moncol, M. Mazúr, M. Valko and J.-H. Choi, *Crystals*, **9**, 336 (2019); <https://doi.org/10.3390/cryst9070336>
27. J. Moncol, M. Mazúr, M. Valko and J.-H. Choi, *Acta Crystallogr. C*, **75**, 616 (2019); <https://doi.org/10.1107/S2053229619005588>
28. J.J. McKinnon, D. Jayatilaka and M.A. Spackman, *Chem. Commun.*, 3814 (2007); <https://doi.org/10.1039/b704980c>